

AD-A086 445

TEL-AVIV UNIV (ISRAEL) SCHOOL OF ENGINEERING F/G 20/4  
ON- THE SPREADING RATE AND STRUCTURE OF A TURBULENT SPOT. (U)  
MAR 80 I WYGNANSKI, J HARITONIDIS AFOSR-77-3275

AFOSR-TR-80-0472

NL

UNCLASSIFIED

1 of 1  
AC  
AD-A086 445

END  
DATE  
FILMED  
8-80  
DTIC

AFOSR-TR-80-0472

3

LEVEL

ADA 086445

Contact/Grant Number

AFOSR-77-3275

ON THE SPREADING RATE AND STRUCTURE OF A TURBULENT SPOT.

I. Wygnanski  
School of Engineering  
Tel-Aviv University

J. Haritonidis  
Department of Aerospace Engineering  
University of Southern California

19 March 1980

Final Scientific Report, 1 March 1979 - 29 February 1980

DTIC  
ELECTE  
JUL 7 1980  
S D C

Approved for public release; distribution unlimited.

Prepared for

AFOSR Bolling Airforce base, Washington D.C. 20332

and

EUROPEAN OFFICE OF AEROSPACE RESEARCH AND DEVELOPMENT  
London, England

DDC FILE COPY

4-73  
80 7 2 037

AIR FORCE OFFICE OF SCIENTIFIC RESEARCH (AFSC)

NOTICE OF TRANSMITTAL TO DDC

This technical report has been reviewed and is  
approved for public release IAW AFR 190-12 (7b).  
Distribution is unlimited.

A. D. BLOSE

Technical Information Officer

SUMMARY

Velocity measurements in the plane of symmetry of a turbulent spot are reported. The number of data points taken at various streamwise locations was adequate to map the ensemble-averaged flow field in a spot at a given instance. These results are compared to velocity taken in laboratory coordinates (i.e., at a given station with variable time), whereupon it is shown that the flow field in the spot depends either on its distance from its origin or on the time elapsed from its initiation. The two variables are not independent, so the flow may be transformed into a time (space) independent problem. The dependence of the spot on the Reynolds number and on the surrounding laminar boundary layer is established. The effects of these parameters on the shape of the ensemble-averaged spot, its size, characteristic celerities, and relative rate of entrainment, are discussed.

Accession For	
Doc. Control	<input checked="checked" type="checkbox"/>
Dist. M.B.	<input type="checkbox"/>
Justification	
By	
Distribution	
Availability Codes	
Dist	Avail and/or special

### INTRODUCTION

Transitional spots have been investigated for several years in view of their role in the generation of a turbulent boundary layer. Pictures of spots, using various techniques of flow visualization, reveal that the spot contains a number of eddies, and thus may be more than just a prototype of a single, large coherent structure. (Fig. 1). Furthermore, an isolated spot in a laminar boundary layer grows indefinitely in both streamwise and spanwise directions, and its dimensions are incomparable with any reasonable boundary layer scales. The substructures within the spot cannot occur entirely at random in view of the universality of the spot's shape and spreading angle. One may postulate that the spot consists either of a large single horseshoe vortex spanning the entire structure on which smaller scales are randomly superimposed, or of a hierarchy of eddies arranged in a particular order, giving the spot its peculiar "arrow-head" shape. The latter assumption is more probable because the origin of the turbulence in the spot was traced to a breakdown of a "Tollmien-Schlichting" wave packet which trails the spot (Wynanski, Haritonidis and Kaplan, 1979). Additional evidence was accumulated by Amini(1978), who investigated the initial stages of the breakdown process and found it orderly at first, with one shaped vortex giving rise to additional  $\Lambda$  shaped vortices, etc. New  $\Lambda$  shaped vortices are perhaps continuously generated at the wing tips of the spot as long as it is embedded in a laminar boundary layer. This generation must be impeded whenever adjacent spots interact to form a turbulent boundary layer, since only a small fraction of the spot survives a prolonged interaction (Zilberman, Wynanski and Kaplan, 1977). The surviv-

ing structure may in fact be  $\Lambda$  shaped but it scales with the turbulent boundary layer thickness. The structure is  $10\delta$  long near the wall,  $3\delta$  long at the outer reaches of the boundary layer; it extends less than  $4\delta$  in the spanwise direction. This structure was convected downstream at  $0.9U_\infty$  (where  $U_\infty$  is the free stream velocity), thus corresponding to the convection velocity of the tip of the arrow in the "arrowhead" transitional structure. The leading edge of the transitional spot moves progressively slower with increasing spanwise distance from the plane of symmetry of the spot, approaching the velocity of the wave packet at its wing-tip. It is possible that a vortex, generated by the breakdown process, accelerates in the streamwise direction until it attains asymptotically its final convection speed of  $0.9U_\infty$ .

If the spot is a prototype of the large coherent eddy in a turbulent boundary layer, its aggregate kinematics and dynamics should be modeled and made amenable to analysis. One possible parameter associated with the kinematics of the spot is the rate at which the spot entrains non turbulent fluid. The spot, being regarded as time dependent, three dimensional structure, can not be easily described mathematically without making some simplifying assumptions. One very powerful and successful method in boundary layer theory is the assumption of similarity, which was applied extensively to the spot by Cantwell, Coles and Dimotakis (1978), hereinafter referred to as CCD. By looking at some characteristic features of the ensemble averaged velocity traces in and around a turbulent spot, CCD concluded that the spot grows conically. The assumption of conical similarity enabled CCD to collapse some characteristic loci in the velocity traces,

measured at two streamwise locations, onto a single curve, thus confirming the concept and defining similarity coordinates and (where  $\eta = Y/U_\infty t$ ;  $\xi = X/U_\infty t$ ;  $t$  being time;  $X$  and  $Y$  are distances in directions parallel and normal to the surface respectively). All quantities are measured from a virtual origin of the flow. In these coordinates, Galilean-invariant particle paths were obtained which enabled the authors to calculate the local rate of entrainment on the plane of symmetry of an ensemble-averaged spot. The particle trajectories led CCD to conclude that there are two vortex structures associated with an ensemble averaged spot. One transverse vortex is located in the centre of the spot, while the other is located near the trailing interface, in the vicinity of the solid surface. Both vortices serve as points of accumulation of the fluid entrained by the spot.

Wynanski, Sokolov and Friedman (1976), hereinafter referred to as WSF, realized that the shape of an ensemble-averaged spot is self-similar, provided the length of the spot at the wall and the maximum height of the spot are used as normalizing length scales. They proceeded to show that the length of the spot should scale linearly with the distance from the measuring station to the location of the disturbance (spark) generating the spot. They also observed that the duration of the spot in its plane of symmetry, scales linearly with the distance of the measuring station from the spark. This scaling provides the transformation between time and space and enables one to interpret measurements made in laboratory coordinates to space coordinates associated with the spot. Schubauer and Klebanoff (1956) suggested that the height of the spot scales approximately as the height of the hypothetical turbulent boundary layer originating at the spark with an

initial thickness equal to the thickness of the laminar boundary layer at that location. The data of WSF agrees with the suggestion made by Schubauer and Klebanoff implying that the laminar boundary layer plays a role in determining the initial shape of the spot and, to some extent, its final height. In fact, it is inconceivable that a transition spot will be totally independent of the laminar boundary layer in which it is embedded and on whose vorticity it must feed.

A detailed comparison between the conical similarity approach of CCD and the experimental investigation of WSF reveals a number of basic differences which should be reconciled if the spot or some part of it is to serve as a prototype large eddy in turbulent boundary layer calculations.

Some of the major differences are :

- (1) According to CCD, the spot grows linearly in every direction. WSF suggest that the streamwise variation of the height of the spot is similar to that of a turbulent boundary layer.
- (2) The conical similarity neglects entirely the effect of the background laminar boundary layer. WSF, as well as Schubauer and Klebanoff (1956), suggest some relationship between the shape of the spot and the laminar boundary layer. To date, the importance of these effects appeared to be secondary, because neither CCD nor WSF considered the consequence of changing the Reynolds number on the growth of the spot.
- (3) The conical similarity approach inherently assumes that every point on the interface of the spot moves with its own characteristic celerity. According to WSF, the celerities of the leading and trailing

interfaces on the plane of symmetry of the spot are constant. Thus, the flow near the interfaces, relative to an observer moving with them, is steady and representative of the physical structure.

The purpose of this investigation was to recheck the hypothesis of conical similarity, of the transitional spot, and to resolve the discrepancies between the interpretation of the measurements reported by CCD and WSF, in particular with regard to the relationship between temporal and spatial rates of growth of the spot. Furthermore, the dependence of some of the characteristic features of the transitional spot on Reynolds number has to be investigated.

### RESULTS AND DISCUSSION

The apparatus used in this experiment, the measuring equipment and the methods of data acquisition and reduction are described in an earlier paper (Wyganski, Haritonidis and Kaplan, 1979) and will not be repeated here.

#### 1. On the Spreading Property of the Spot

Figure (2) shows a typical record of velocity perturbation measured at a station  $X_m - X_s = 1100\text{mm}$  downstream of the spark and  $1400\text{mm}$  downstream of the leading edge of the plate, (the distance from the hypothetical origin of the flow is  $X_m - X_o = 1030\text{mm}$ ). The free stream velocity  $U_\infty$  was  $10\text{m/sec}$ . The abscissa in this figure is time, starting  $70\text{msec}$  after the occurrence of the spark and ending  $204.8\text{msec}$  later. Each trace in the figure repre-

interfaces on the plane of symmetry of the spot are constant. Thus, the flow near the interfaces, relative to an observer moving with them, is steady and representative of the physical structure.

The purpose of this investigation was to recheck the hypothesis of conical similarity, of the transitional spot, and to resolve the discrepancies between the interpretation of the measurements reported by CCD and WSF, in particular with regard to the relationship between temporal and spatial rates of growth of the spot. Furthermore, the dependence of some of the characteristic features of the transitional spot on Reynolds number has to be investigated.

### RESULTS AND DISCUSSION

The apparatus used in this experiment, the measuring equipment and the methods of data acquisition and reduction are described in an earlier paper (Wyganski, Haritonidis and Kaplan, 1979) and will not be repeated here.

#### 1. On the Spreading Property of the Spot

Figure (2) shows a typical record of velocity perturbation measured at a station  $X_m - X_s = 1100\text{mm}$  downstream of the spark and  $1400\text{mm}$  downstream of the leading edge of the plate, (the distance from the hypothetical origin of the flow is  $X_m - X_o = 1030\text{mm}$ ). The free stream velocity  $U_\infty$  was  $10\text{m/sec}$ . The abscissa in this figure is time, starting  $70\text{msec}$  after the occurrence of the spark and ending  $204.8\text{msec}$  later. Each trace in the figure repre-

sents velocity measured at a different elevation above the plate from 1mm above the surface to 25.4mm from the wall. The velocity history across the entire cross section of the spot is thus recorded for every realization. The local velocity prevailing in the laminar flow is subtracted from each record in order to facilitate the presentation. When 200 events are ensemble-averaged, the turbulent (high frequency) fluctuations occurring at random during each realization disappear, leaving a fairly smooth record of average perturbation velocity during a passage of a spot (Fig. 3).

Records similar to Figure 3 were presented by WSF and CCD. The ensemble-averaged velocity record marking the spot can be characterized by a defect in velocity at the outer edge of the boundary layer and an excess of velocity near the surface. The boundary of the spot may be represented over most of its length by a perturbation contour of  $\pm 2\% U_\infty$  with the exception of a small region near the surface at the rear-end of the spot. In this region, the spot boundary crosses the maximum positive velocity perturbation. CCD suggested that each record was well represented by several straight-line segments intersecting at points labelled A through G (see Fig. 12 in CCD). Although it is not felt that this representation is justified, nor is it important for the discussion that follows, some of the corresponding points are marked in Figure 3 for the purpose of orientation. From the record shown, one may choose four characteristic features on the boundary of the spot and determine the time of their occurrence. These points mark the following locations:

1. The leading edge of the spot at the surface.
2. The most forward-reaching position of the leading interface (the over-

hang).

3. The location of the maximum height of the spot.
4. The trailing edge of the spot at the surface.

By repeating the measurement at numerous streamwise locations on the plane of symmetry of the spot, the points labelled 1 through 4 occur at different times which are determined by the location of the probe. These loci are plotted in  $X, t$  coordinates, (Fig. 4), in a manner suggested by CCD. Data from 9 measuring stations is shown in Figure 4 for streamwise locations varying from 800 to 1500mm downstream of the spark. The loci marked may be connected by straight lines, whose slopes represent the celerity of the particular features chosen. The celerity of loci 1 and 2 is  $0.89U_\infty$  and of locus 3 is not appreciably different. The celerity of locus 4 is  $0.57U_\infty$ . Loci 1, 2 and 3 are situated on the leading interface of the spot. Thus, the equality of their celerity implies that the entire leading interface moves downstream with a constant velocity independent of  $Y$  ( $Y$  being the distance from the surface). Furthermore, the inclination and shape of the leading interface does not vary with increasing distance from the spark. The contours  $U - U_{LAM}/U_\infty = -0.02$  which represent the interface of the spot outside the laminar boundary layer are shown in Fig. 4b. This determination of the spot's boundary was first used by Coles and Barker (1975) and is repeated here for the sake convenience; a detailed comparison between this criterion and the actual determination of the turbulent-non-turbulent interface is discussed by WSF. One may deduce from Fig. 4b that the boundaries of adjacent spots measured 10 cm apart are parallel reinforcing the notion that the celerity of the trailing inter-

faces in the X direction is locally independent of Y. In order to compare the celerity of the trailing interface over a long downstream distance, one has to account for the growth of the spot in the Y direction as well. It should be remembered, however, that the coordinates used in Fig. 4b accentuate the height of the spot which is physically a very flat structure.

The present results are in agreement with the findings of WSF, who measured the convection velocity of the leading interface locally but do not agree with the conical similarity assumption proposed by CCD. If the conical similarity in the form suggested by CCD were to prevail, the lines passing through loci 1, 2, 3 and 4 would converge to a common origin; thus, the celerity of 2 should have been larger than 1 and the latter's larger than 3. Only the celerity of 4 is significantly different from the celerities of other three loci. The difference between the celerities of the leading and trailing interface is associated with the spatial growth of the spot. In fact, the length of the spot almost doubles between  $X_m = 800\text{mm}$  and  $X_m = 1500\text{mm}$  corresponding the two extreme locations shown in Figure 4. The lines connecting loci 1 and 4 intersect at  $t_0 = 12\text{msec}$  and  $X_0 - X_s = 70\text{mm}$  which may represent the virtual origin at the wall. However, since loci 2 and 3 do not intersect 4 at the same point as 1, there is no uniquely defined virtual origin for the spot. One may chose the intersection of 2 and 4 for the virtual origin because these loci represent the extreme streamwise extent of the spot, although locus 2 is at the edge of the laminar boundary layer. It is known (Kovasznay, et al 1962) that the breakdown to turbulence originates at the outer part of the laminar boundary layer, favouring perhaps the choice of 2. One may also chose the origin

of the spot at the intersection of locus 3 with either one of the principal axes ( $t$  or  $X$ ). Locus 3, if it were to exist in a single event, would represent a singular point at the intersection of the leading and trailing interfaces which are moving downstream at different velocities. Since locus 3 has a celerity of the leading interface it has also to move outwards in order that the angle between the trailing interface and the surface be preserved. One may use the location of the spark as the origin of the flow or the intersection of any locus on the interface of the spot with one of the principal axes. In the following discussion,  $X_0$  and  $t_0$  was chosen using the intersection of 1 and 4 but this choice is arbitrary and has no appreciable influence on the results.

In the absence of the conical property, the similarity coordinates  $\xi = X/U_\infty t$  and  $\eta = Y/U_\infty t$  (where  $X$ ,  $Y$  and  $t$  are independent variables) suggested by CCD are not appropriate, implying that the spot cannot be scaled by a single length scale ( $U_\infty t$ ). Nevertheless, it is still possible that every characteristic feature of the spot (locus 4) is convected downstream with a constant celerity so that the ratio  $(X_m - X_0)/U_\infty(t_m - t_0)$ , representing this feature and its own virtual origin be always constant. This could imply that there is only one scaling factor relating measurements made in laboratory coordinates (i.e. at fixed  $X$  but varying time) to spatial measurements made at a given time. The latter would be an equivalent of a photographic record showing the instantaneous flow in and around the spot. Having measured the ensemble averaged velocity distribution at 9 streamwise locations, one can compare the temporal velocity record taken at any location in the flow during the passage of the spot, with the velocity measured

at a given time at all 9 locations. The "X" symbols shown in Figure 5 represent velocity perturbations observed 172msec after the initiation of the spot. The first "X" symbol on the left side of Figure 5a represents the velocity at the furthest streamwise location (i.e.  $X - X_0 = 1430\text{mm}$ ) at the particular time chosen; at that time the spot was about to arrive at this location. The trailing edge of the spot near the surface, at that point in time, occurs roughly at  $X - X_0 = 880\text{mm}$  downstream of the hypothetical origin. The solid lines shown in Figures 5a-c represent the temporal record of ensemble averaged-perturbation velocity at three streamwise positions ranging from 830mm to 1430mm downstream of the origin. The comparison was made after the temporal record was multiplied by  $1.1 U_\infty / (X_m - X_0)$  where  $U_\infty$  and  $(X - X_0)$  respectively, are the velocity of the free stream (in this case  $U_\infty = 10 \text{ m/sec}$ ) and the distance of the measuring station from the origin. The agreement between the two types of measurement is good ahead of the spot (i.e., before the leading interface) and inside the turbulent spot. Only behind the spot, (i.e., after the trailing interface) and inside the laminar boundary layer, the temporal record of velocity adjusts somewhat slower to its unperturbed conditions than the spatial velocity distribution. It implies that, in this region, the flow is sensitive to the characteristics of the laminar boundary layer surrounding the spot.

It is important to note from Figure 5 that the dimensionless length of the spot at a given time is proportional to the dimensionless duration of the spot at a given measuring station, i.e.

$$\frac{\ell}{U_{\infty}(t_m - t_o)} \propto \frac{\Delta t U_{\infty}}{(X_m - X_o)}$$

where

$\ell$  is the length of the spot

$\Delta t$  is the duration of the spot

$t_m$  is the time of measurement

$X_m$  is the location of measurement

Consequently,  $X$  and  $t$  are not independent variables in this flow. Since it is more convenient to use laboratory coordinates at which  $X$  is fixed, the similarity time scale of the problem becomes  $(X_m - X_o)/U_{\infty}$  by which temporal velocity records obtained at any measuring station should be scaled. This scale applies to every measuring station as long as the Reynolds number at the location of the spark is fixed.

The spot also grows in the direction perpendicular to the wall, as may be seen from the three temporal records shown in Figure 5. At  $X_m - X_o = 1430\text{mm}$  the spot extends beyond  $Y = 25.4\text{mm}$  while at  $X_m - X_o = 830\text{mm}$  it's tip, as it may be detected from the perturbation in velocity, does not extend much beyond  $19\text{mm}$ , resulting in some discrepancy between the spatial and temporal velocity distributions at large values of  $Y$ . Schubauer and Klebanoff (1956) suggested that the rate of growth of the spot in the  $Y$  direction is proportional to the growth rate of a turbulent boundary layer developing

downstream of the spark, with an initial thickness equal to the thickness of the laminar boundary layer at the location of the spark. This suggestion agreed with the results of WSF and hence was tried in the present context. It seems reasonable to assume for this purpose that the turbulent boundary layer-thickness may be represented by a power-law, thus  $\delta_T = 0.37 (X_m - X_1)^{4/5} (\nu/U_\infty)^{1/5}$  where  $\delta_T$  is the thickness of a turbulent boundary layer and  $X_1$  is determined by equating  $\delta_T = \delta_{LS} = 5X_S^{1/2} (\nu/U_\infty)^{1/2}$  where  $X_S$  is the location of the spark from the leading edge of the plate and  $\delta_{LS}$  represents the laminar boundary layer thickness at the spark. For  $U_\infty = 10\text{m/sec}$  and  $X_S = 300\text{mm}$  from the leading edge  $X_1$  is 80mm upstream of the spark.

Scaling the distances measured from the wall by  $\delta_T$  and the time by the characteristic time scale  $(X_m - X_0)/U_\infty$  at the measuring station of the perturbation contour  $U - U_{LAM}/U_\infty = \pm 0.02$  is plotted in Figure 6. The various symbols shown in the figure represent different measuring stations starting 800mm downstream of the spark and ending 700mm further downstream. The collapse onto a single curve is fairly good, indicating that the variables chosen to scale the spot are reasonable. Since both positive and negative perturbation contours are shown, the concentration of symbols near the surface is due to the fact that between 2-4mm from the plate, the ensemble averaged velocity perturbation becomes first positive then negative and then positive again. The positive perturbation contours are marked by open symbols while the negative ones are marked by full ones; the former are hardly distinguishable in view of the large number of symbols piling one on top of the other. Assuming that the origin of the spot coincides

with the location of the spark and neglecting the thickness of the laminar boundary layer at this location, (i.e., letting  $X_0 = t_0 = \delta_{LS} = 0$ ) does not have a large adverse effect on the similarity considerations (Fig. 6b). By choosing the intersection of locus 3 (Fig. 4) with the time axis ( $t_0 = 12$ ;  $X_0 = 0$ ) as the origin of the spot, the similarity of the data is improved near the outer tip of the spot but is somewhat degraded near locus 2, (Fig. 6c). The differences are not sufficiently significant to warrant a preference of one choice of virtual origin upon another. The perturbations  $U - U_{LAM}/U_\infty = \pm 0.1$  are plotted in Figure 7 to underline the fact that the entire velocity perturbation field inside the spot scales correctly with the chosen parameters and not just the spot boundaries. The separation distance between the positive and negative perturbations is now larger so that each contour can be clearly visible. If there is any significant deviation from similarity, it occurs at the first two stations where the spot may not have yet attained its final shape. WSF also observed that the spot attains a characteristic terminal shape approximately 700mm downstream of the disturbance for similar experimental conditions (i.e.,  $U_\infty = 10\text{m/sec}$   $X_s = 30\text{ cm}$  from leading edge).

The same data, when plotted in the coordinates of CCD [i.e.,  $\xi = (X_m - X_0)/(t - t_0)U_\infty$ ;  $\eta = y/(t - t_0)U_\infty$ ] does not collapse as well onto a single curve (Fig. 8). This is particularly true at the outer part of the laminar boundary layer, where an increase in downstream distance causes an apparent shrinkage of the spot. Figure 8 shows that the height of the "overhang" (i.e., the most forward portion of the leading interface) varies by 50% when one compares data taken at  $X_m - X_0 = 830\text{mm}$  with data taken at

$X_m - X_o = 1430\text{mm}$ . As discussed subsequently, this could lead to erroneous interpretation of the rate of entrainment at the outer part of the leading interface (segment 2 to 3 in Figure 4). Since time is not an independent variable in this problem, one may express the boundary layer thickness used for scaling  $Y$  in terms of  $U_\infty(t-t_o)$  and obtain as good a collapse of the data as in Figure 6. This result reaffirms the fact that the problem is independent of either time and space and is not invariant under a Galilean transformation.

We may now examine the flow at a particular station by plotting the data in a coordinate system:

$$\bar{X} = U_\infty(t_m - t_o)/(X_m - X_o); \bar{Y} = Y/\delta \text{ where } (\delta = \delta(X_m - X_o))$$

knowing that this representation is valid for the entire flow field at any given time. Contours of constant velocity perturbation  $(U - U_{\text{LAM}})/U_\infty = C$  imply that the spot is represented by a family of closed loops of velocity defect riding above contours representing an excess of velocity, (Fig. 9). The velocity defect region coincides with the turbulent region in the spot, while the excess region has its maximum near the rear of the spot and is trailing behind it. The maximum perturbation velocity associated with the spot is approximately  $+30\%U_\infty$ .

Assuming that the ensemble-averaged flow in the plane of symmetry of the spot is two dimensional (see WSF), a stream function may be defined as:

$$\psi/U_\infty\delta = g(\bar{Y}, \bar{X})$$

where  $\delta$  is a function of  $X$ .

This function depends on the speed of a uniformly moving observer because the proportionality constant relating time to length depends on the reference velocity chosen. It was deduced from Figure 5 that  $U_{\infty}(t_m - t_o)/(X_m - X_o) = 0.9$ , but  $(U_{\infty} - U_o)(t_m - t_o)/(X_m - X_o)$  is also a constant which can be used for transforming length scale to time scale. Thus, the streamline pattern in a frame of reference moving with  $U_o = 0.89U_{\infty}$  represents the flow relative to the leading interface and the pattern moving at  $U_o = 0.57U_{\infty}$  represents the flow relative to the trailing interface. The perturbation velocity contour of  $\pm 2\%$  showing the borders of the spot is also sketched, (Fig. 10a,b), to indicate the amount of fluid entrained by the spot. The total entrainment can be divided as shown in Table I.

Table I

	Segment	Present	WSF	Present
Leading interface	<u>1</u> - <u>2</u>	16%	10%	13%
Leading interface	<u>2</u> - <u>3</u>	16%	13%	13%
Trailing interface	<u>3</u> - <u>4</u>	68%	77%	74%
$U_{TE}/U_{\infty}$	-	.57	.5	.5

The amount of fluid entrained by the trailing interface appears to be lower than estimated from previous measurements (WSF). Most of the difference results from an increase in the celerity of this interface relative to the celerity measured by WSF rather than from differences in the shape of the spot or the flow field surrounding it. When the present streamline pattern was recomputed for  $U_{TE}/U_{\infty} = 0.5$ , the agreement with previous results was better. CCD claim that the outer part of the forward interface is entirely passive. According to the present observations, this region entrains as much fluid as segment 1-2 near the wall. However, segment 2-3 is approxi-

mately three times longer than segment 1-2 and thus the rate of entrainment per unit length of an average leading interface is stronger near the wall. The apparent inactivity of the outer part of the forward interface observed by CCD may be attributed in part to the assumption that  $\delta \propto U_{\infty} t$  which has been shown to be inaccurate (Fig. 8). The other possible reason for the discrepancy may stem from the fact that CCD considered the problem to be dependent on both  $X$  and  $t$ , while actually it depends on one of these variables only.

## 2. The effect of Reynolds number

The laminar boundary layer which provides the medium for the generation of the spot was not considered in the previous discussion. The thickness of this layer introduces another length scale, the effect of which was never carefully investigated because most of the detailed experiments were carried out at one free stream velocity and because the perturbation generating the spot was fixed in space.

When the experiments discussed in the previous section were repeated at a free stream velocity of 19 m/sec, some differences were noticed. By plotting the same features, as in Figure 4, it appears that:

- (i) the relative celerity of the leading interface remained unchanged, (i.e.,  $U_{LE} = 0.89U_{\infty}$ ).
- (ii) The trailing interface slowed down to  $U_{TE} = 0.515U_{\infty}$
- (iii) The various virtual origin of the flow moved upstream, (Fig. 11).

The reduction in the celerity of the trailing interface was significant and could not be attributed to experimental error. The same trend was observed in the transitional pipe flow, whereupon the velocity of the trailing edge of the slug decreased monotonically with increasing  $Re$  (Wyganski and Champagne, 1973). Since the difference in the celerity of the leading and trailing interfaces is associated with the rate of growth of the spot, the latter was investigated in detail near the surface of the plate. The actual length of the spot near the solid surface can be determined by having two hot-wire probes separated by a distance corresponding to the spot length. Whenever the separation distance is correct, the trailing interface as seen by the first probe occurs simultaneously with the leading interface seen by the second probe. Because this determination is possible in a statistical sense only, one may determine the probe separation from ensemble-averaged data of a single wire and thus avoid undesirable effects of probe interference. Repeating the same measurement at numerous distances downstream of the spark, it appears that the spots grow linearly with  $X$  ( $X$  being the distance between the leading edge of the spots and their virtual origin on the surface) and their rate of growth  $dL/dX$  can be plotted for various Reynolds numbers based on the conditions at the spark (Fig. 12). Two spark positions were considered; one at  $X_s = 300\text{mm}$  and the other at  $X_s = 600\text{mm}$  from the leading edge while the velocities ranged from 5 to 19m/sec. The rate of growth of the spot depends on  $Re$  and it doubles as  $Re_{\delta_s^*}$  at the spark location is increased from 500 to 1500. The celerity of the trailing interface is also plotted in Figure 12, indicating a continuous reduction of  $U_{TE}$  with increasing  $Re_{\delta_s^*}$ . In the range of  $Re$  considered, the celerity of the trailing interface varies from

$0.62U_{\infty}$  to  $0.5U_{\infty}$ . The celerity of the leading interface is independent of  $Re_{\delta_s^*}$  at the spark. Two data points taken from other experiments are shown in Figure 12 for comparison. One was taken from CCD, who had a slight pressure gradient on their plate; the other was measured by Zilberman, (private communication), in the wind tunnel facility at Tel-Aviv University.

The spanwise rate of growth of the spot is hardly dependent on  $Re$  at the spark, as may be observed from the slope of the lines drawn in Figure 13. The maximum spanwise rate of spread corresponds to an angle of  $10^\circ$  while the minimum to  $9.3^\circ$ . The location of the hypothetical origin of the flow in the X-Z plane depends on the free stream velocity more than it does on the location of the spark and does not simply scale with  $Re_{\delta_s^*}$ . For all cases considered,  $Re_{\delta_s^*} > 450$  which is regarded as the critical Reynolds number below which all small disturbances should decay. The initial lateral growth of the spot is slow at low values of  $Re_{\delta_s^*}$ , but the asymptotic state appears to be independent of Reynolds number.

In attempting to scale the spot geometry, one has to consider three apparent origins of the flow:

- (1) relating time to streamwise distance.
- (2) relating the local boundary layer thickness to the initial thickness at the spark.
- (3) relating the rate of growth in the spanwise direction to the velocity and Reynolds number of the flow.

The rate of growth of the spot in all three directions is also different:

- (1) The length of the spot (in the X direction) increases linearly with downstream distance and its rate of growth ( $dL/dx$ ) increases almost linearly with  $Re_{\delta_s}^*$ .
- (2) The height of the spot (in the Y direction) increases with X at a rate similar to the growth of the turbulent boundary layer thickness. Assuming a power law relationship, it implies that for a given free stream velocity, the height of the spot increases proportionally to  $X^{0.8}$ . This rate of growth is weakly dependent on  $Re$ .
- (3) The width of the spot (in the Z direction) increases linearly with X; irrespective of  $Re$ , provided the latter is large enough.

Thus, the spot cannot be described as a universally self similar structure growing conically from a single origin.

The constancy of the relationship between temporal and spatial velocity records applies equally well to different Reynolds numbers as it did to the data shown in Figure 5. The proportionality constant, however, depends on  $Re$  because the streamwise rate of growth of the spot is dependent on  $Re_{\delta_s}^*$  and the difference between the celerity of the leading and trailing interface also depends on  $Re$ .

The borders of ensemble-averaged spots, are plotted in Figure 14a,b using the similarity variables suggested previously for  $U_\infty = 6\text{m/sec}$  and  $U_\infty = 19\text{m/sec}$ . The shapes of the spots are self similar for each  $Re_{\delta_s}^*$ , proving

the proper choice of the scaling parameters. In Figure 14b the perturbation contours  $(U-U_{LAM})/U_{\infty} = -2\%$ ;  $-10\%$ ;  $-20\%$  are plotted in order to show again that the entire perturbation flow field associated with the passage of the spot scales correctly with the chosen variables. There are, however, some obvious Reynolds number effects:

(i) The maximum height of the spot (point B) in Figure 14a is approximately  $0.75\delta_T$  while in Figure 14b it is  $0.9\delta_T$ . For  $Re_{\delta_s^*} = 1500$ , the maximum height of the spot is  $0.95\delta_T$ . The temporal (or spatial) position at which the spot attains its maximum height is given by:  $U_{\infty}(t-t_0)/(X_m-X_0) \approx 1.22$  for all Re considered.

(ii) The height of the "overhang" (i.e., the most forward location on the spot boundary) does not depend on Re and is found at  $Y/\delta \approx 0.26$ , but its streamwise location depends weakly on Re and occurs  $1 \geq U_{\infty}(t-t_0)/(X_m-X_0) \geq 0.94$  in the range of Re considered.

(iii) The most rearward  $-2\%$  velocity perturbation (point "C" in Figure 14a) moves closer to the surface with increasing  $Re_{\delta_s^*}$  (from  $Y/\delta = 0.2$  in Figure 14a to  $Y/\delta = 0.15$  in Figure 14b), while at the same time occurring at larger values of  $U_{\infty}(t-t_0)/(X_m-X_0)$ .

The effect of  $Re_{\delta_s^*}$  on the flow field in the spot is clearly visible in Figure 15a,b where contours of velocity perturbation are plotted for  $X_m-X_0 \approx 1000\text{mm}$ . The Reynolds numbers considered are identical to the ones shown in Figure 14. The region of strongest defect of velocity occurs in Figure 15a at an elevation corresponding to  $1/3$  of the total height of the spot and  $1/2$  of its length. The corresponding location in Figure 15b occurs at an elevation of  $22\%$  of the height of the spot and  $30\%$  of its length

(i.e., closer to the leading interface of the spot). The relative height of the "calmed" region behind the spot extends 30% of the spot height in Figure 15a and only 20% of the height in Figure 15b. The streamwise distance between the highest velocity defect region and maximum velocity excess region is also increased with increasing  $Re_{\delta_s}^*$ .

The effect of Reynolds number on the streamline pattern is less pronounced than on the velocity perturbation contours because the latter represents an integral effect. One may estimate, however, the effect of  $Re$  on the relative amounts of the fluid entrained by the different regions of the spot. The dependence of entrainment on  $Re$  is shown in Table II.

Table II

$Re_{\delta_s}^*$	$U_\infty$ m/sec	$\delta_s$ mm	Segment <u>1</u> - <u>2</u>	Segment <u>2</u> - <u>3</u>	Segment <u>3</u> - <u>4</u>
			Leading interface		Trailing interface
600	6	4.33	26%	9%	65%
780	10	3.35	16%	16%	68%
1060	19	2.44	10%	15%	75%
1520	19	3.45	8%	15%	77%

The relative rate of entrainment of the trailing interface increases with  $Re_{\delta_s}^*$ . The effect is attributed in part to the reduction in the celerity of the trailing interface and in part to an increase in relative length to this interface. The two effects, however, may not be independent.

The amount of fluid entrained near the wall at the leading interface (segment 1-2) is reduced by increasing  $Re_{\delta_s^*}$ , in spite of the fact that neither the contact area nor the celerity of this segment is affected significantly by  $Re$ . The primary reason for the reduction in the rate of entrainment is the change in the thickness of the laminar boundary layer surrounding the spot. Since the leading interface is convected at a constant  $U_{LE}$ , fluid is entrained by segment 1-2 as long as the local velocity  $U < U_{LE}$  and the value of  $\int_0^y (U - U_{LE}) dy$  increases by increasing the thickness of the laminar boundary layer.

The relative amount of entrainment by segment 2-3 appears to be constant for  $Re_{\delta_s^*} > 800$ , but it is quite a lot less for  $Re_{\delta_s^*} = 600$ . The  $Re$  at the location of the perturbation in the experiment of CCD was estimated to be equal to  $Re_{\delta_s^*} = 430$ , (in part due to the slightly favourable pressure gradient on the surface). This  $Re$ , being lower than any considered in the present experiment, may be responsible in part for the conclusion of CCD that segment 2-3 does not entrain any fluid at all. In spite of the fact that the entrainment into an ensemble-averaged spot is discussed in terms of  $Re$ , the latter may not necessarily be the only parameter governing the distribution entrainment around the spot. In fact, the ratio between the height of the spot and the thickness of the laminar boundary layer can be considered as an independent parameter of the flow. This ratio was considered implicitly in scaling the boundaries of the spot by assuming the initial thickness of the latter (at the location of the spark) to be equal to the thickness of the laminar boundary layer.

### 3. The structure of the spot

Thus far, the entire discussion of the shape of the spot and the rate at which it entrains non turbulent fluid was based on ensemble-averaged data. The averaging process eliminates all fluctuations which occur randomly within the spot and gives the impression that its boundaries are smooth. The picture of a "tagged" spot (Fig. 1) indicates clearly that the free interface between the turbulent and non turbulent fluid is deeply corrugated, implying that the spot contains a finite number of large coherent structures. A record of the streamwise component of the velocity perturbation taken at  $U_{\infty} = 6\text{m/sec}$  and  $X_m - X_0 = 940\text{mm}$  is shown in Figure 16. Each velocity record was low-pass filtered digitally and replotted on the same figure for comparison, after being slightly displaced in the vertical direction. The filtering operation did not remove the low frequency oscillations which are coherent across the entire spot and can be followed from the solid surface to the outer interface. Contours of constant velocity perturbation were replotted from the records shown in Figure 16 using the same techniques as for the ensemble-averaged data, (Fig. 9). The velocity perturbation contours indicate that the flow for the individual realization can still be described by a region of excess velocity near the surface and a region of velocity defect further away. The largest perturbation of velocity is  $U - U_{\text{LAM}}/U_{\infty} = \pm 0.4$ , representing an increase of 30% over the ensemble-averaged data.

The boundaries of the spot are deeply corrugated and resemble the picture shown in Figure 1. One may distinguish roughly 5 cellular eddy struc-

tures in the spot which are coherent across its entire height. These eddies are separated by deep crevassies in which non turbulent fluid can be trapped. Wygnanski, Haritonidis and Kaplan (1979) suggested that oscillations in the "Tollmein-Schlichting" frequencies persist inside the spot even on its plane of symmetry. Thus, if the spot could be regarded as a packet of breaking waves, it would have been natural for it to contain a finite number of large coherent structures rather than a single spanwise vortex. The hierarchy of breakdown may be inferred from Figure 16, whereupon the first wave to break is the wave forming the leading interface of the spot and the last wave forms a part of its trailing interface. This outlook could also explain the reason for the linear rate of growth of the spot and its dependence on  $Re$ . Since the relationship between the wave packet which follows the spot and the sub-structure inside the spot was not yet positively identified, the above mentioned explanation should be regarded as highly tentative for the time being.

CCD suggested that the spot entrains non turbulent fluid by a process they called "nibbling" namely the propagation of a thin interface into the non turbulent fluid by viscous diffusion of vorticity. The "nibbling" process is dominant whenever the interface is fairly smooth. In the case of the individual spot, the non turbulent fluid may be engulfed between adjacent crests of the breaking waves, allowing the relatively slow process of diffusion by smaller scales to act within the folds of the large eddies. The actively entraining surface area is greatly increased by the engulfment process, enabling the spot to grow rapidly with downstream distance. The "nibbling" process suggested by CCD, on the basis of ensemble-averaged

data, would require unrealistically large diffusion rates to explain the rapid rate of growth of the spot with time or distance from its origin.

### CONCLUSIONS

It is established that the size of the transitional spot in a Blasius boundary layer depends either on its distance from the source or on the time elapsed from its initiation. The two variables, however, are not independent as long as the free stream velocity and the location of the perturbing source are held constant. Relative to an observer moving with speed of an interface of an ensemble-averaged spot, the flow field in his immediate vicinity, is steady causing the streamlines to coincide with particle trajectories. The rate of growth of the spot and the location of its apparent origin, differs for each of the three principle directions. The dependence of the size and shape of the spot on the Reynolds number and on the thickness of the surrounding laminar boundary layer, limits the usefulness of a single, similarity transformation.

Finally, the physical process of entrainment can not be satisfactorily explained from an ensemble-averaged picture of the spot.

ACKNOWLEDGEMENT

This research was sponsored in part by the U.S. Air Force Office of Scientific Research under grants 76-3094, 77-3275. The experiments were carried out at the University of Southern California, but most of the data processing was done at Tel-Aviv University. Special acknowledgement is due to Dr. M. Gad-el-Hak of Flow Research for the dye pictures shown in Figure 1.

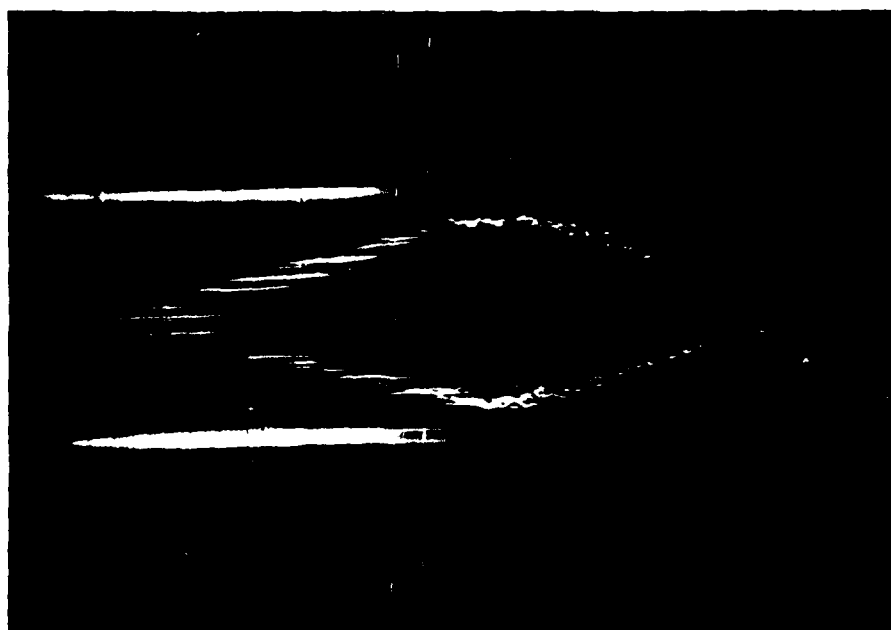
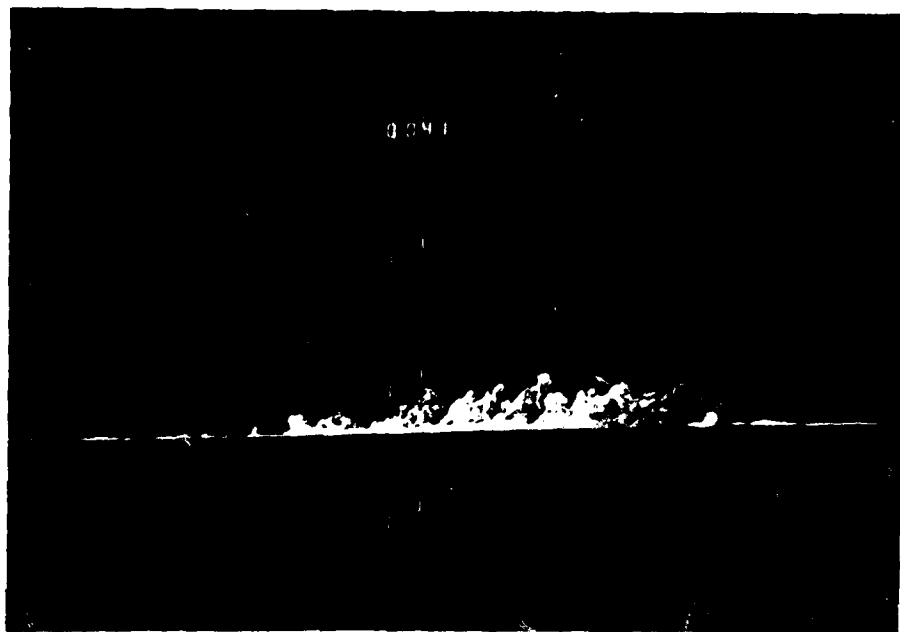
References

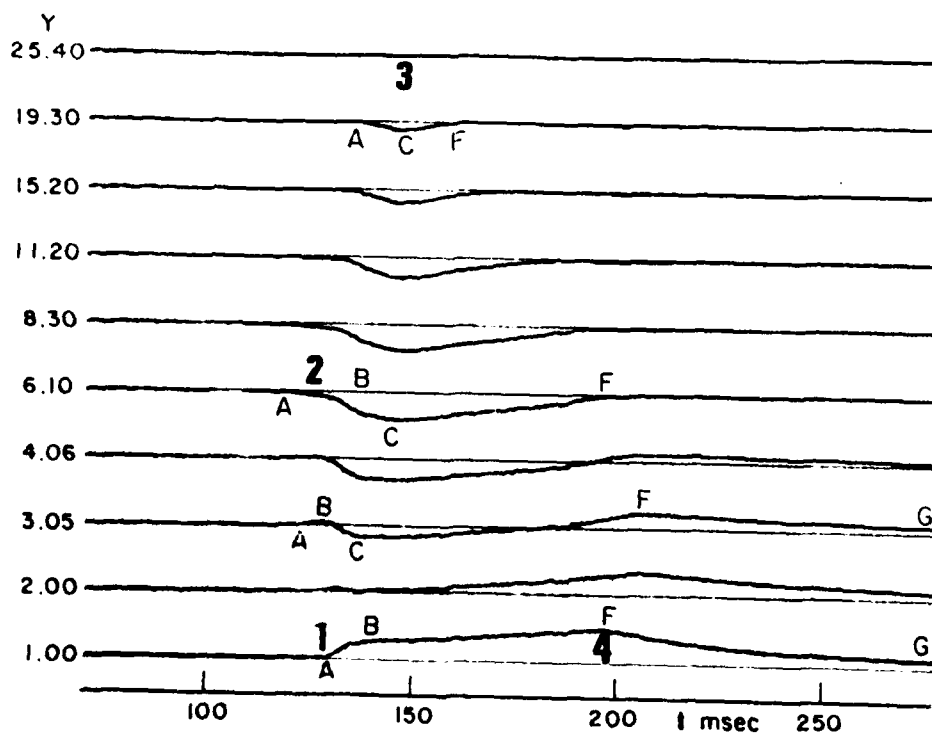
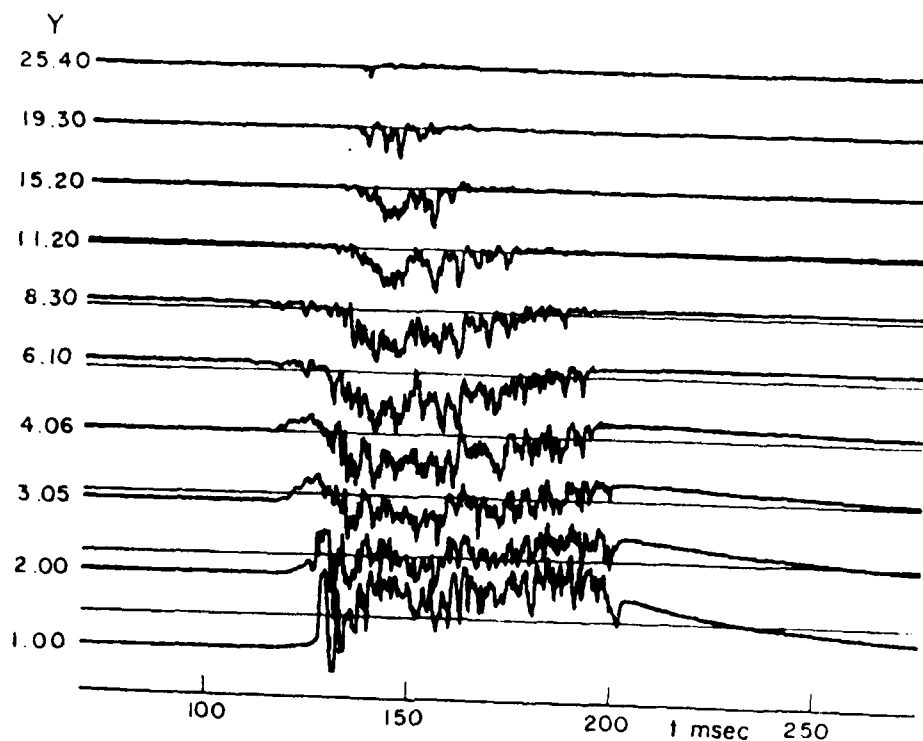
1. Amini, J., (1978) Ph.D. Thesis, Institut de Mecanique de Grenoble (France) To be published in Phys. of Fluids.
2. Cantwell, B., Coles, D., Dimotakis, P. (1978) JFM, 87, 641.
3. Coles, D. and Barker, S.J. (1975) in Proceedings of Project SQUID Workshop on Turbulent Mixing in Non-reactive and Reactive Flows, edited by S.N.B. Murthy, Plenum Press, New York.
4. Kovasznay, L.S.G., Komoda, H. and Vasudeva, B.R. (1962) Proc. of Heat Transfer and Fluid Mechanics Institute, Stanford University Press.
5. Schubauer, G.B. and Klebanoff, P.S. (1956) NACA Report 1289.
6. Wygnanski, I., Sokolov, M., Friedman, D., (1976) JFM 784, 785.
7. Wygnanski, I., Haritonidis, J., Kaplan, R.E. (1979), JFM 92, 505.
8. Wygnanski, I., Champagne, F.H. (1973), JFM 59, 281.
9. Zilberman, M., Wygnanski, J., Kaplan, R.E. (1979), Phys. of Fluids, 20,S 258..

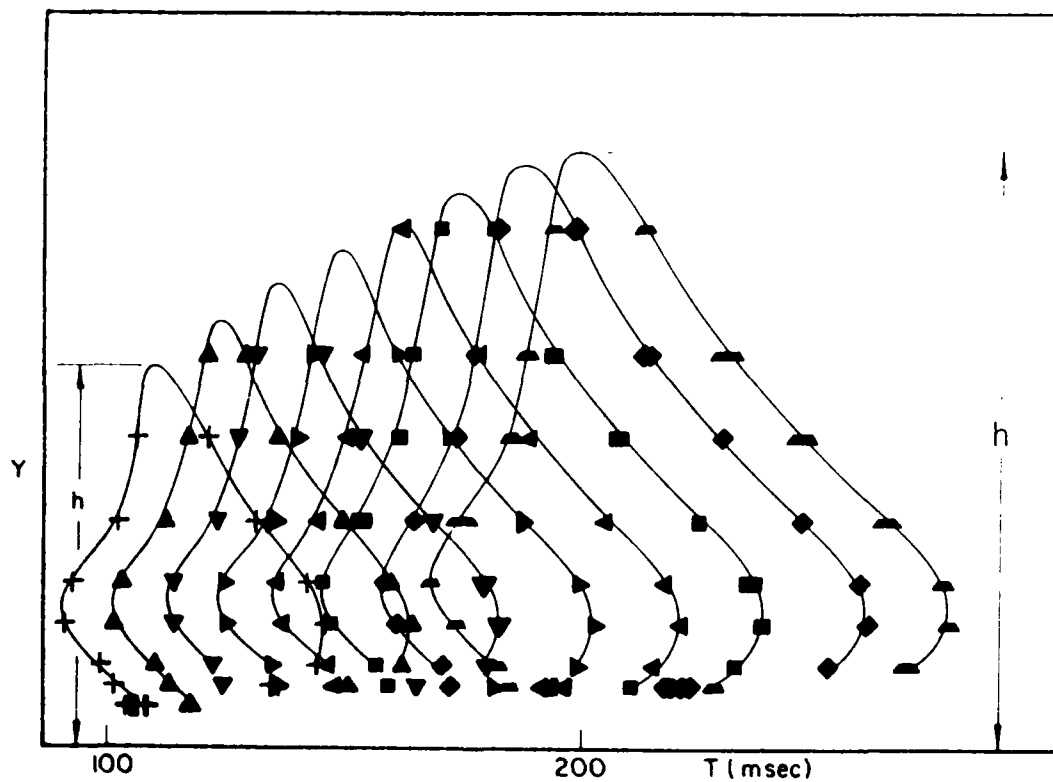
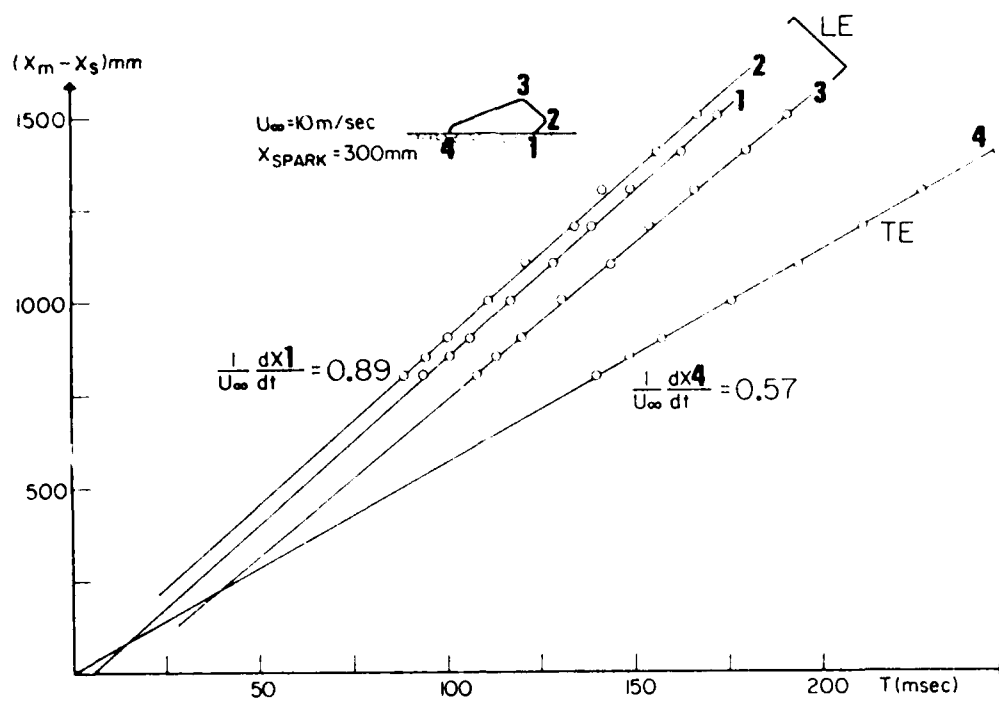
# LIST OF FIGURES

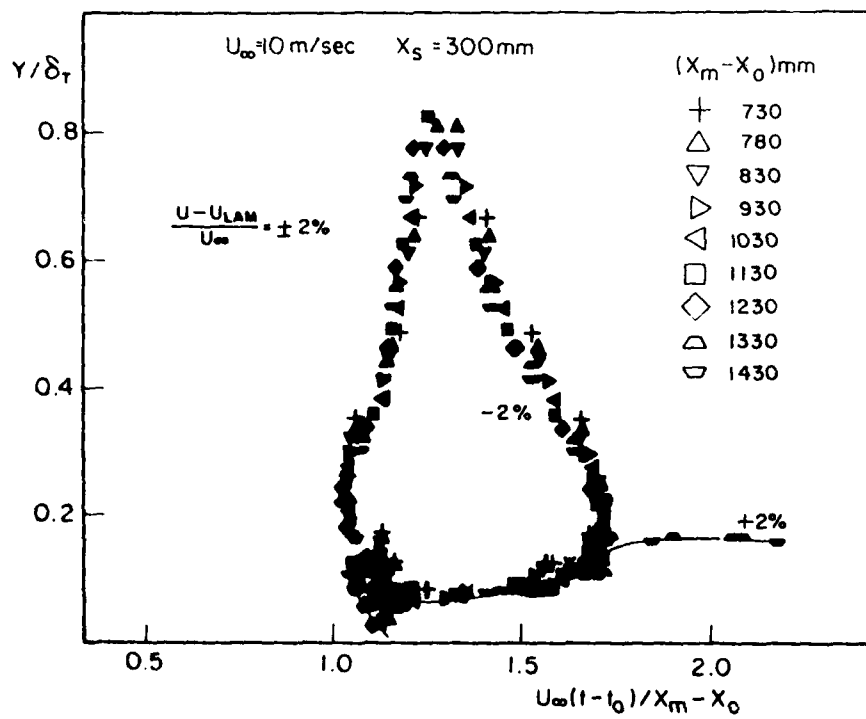
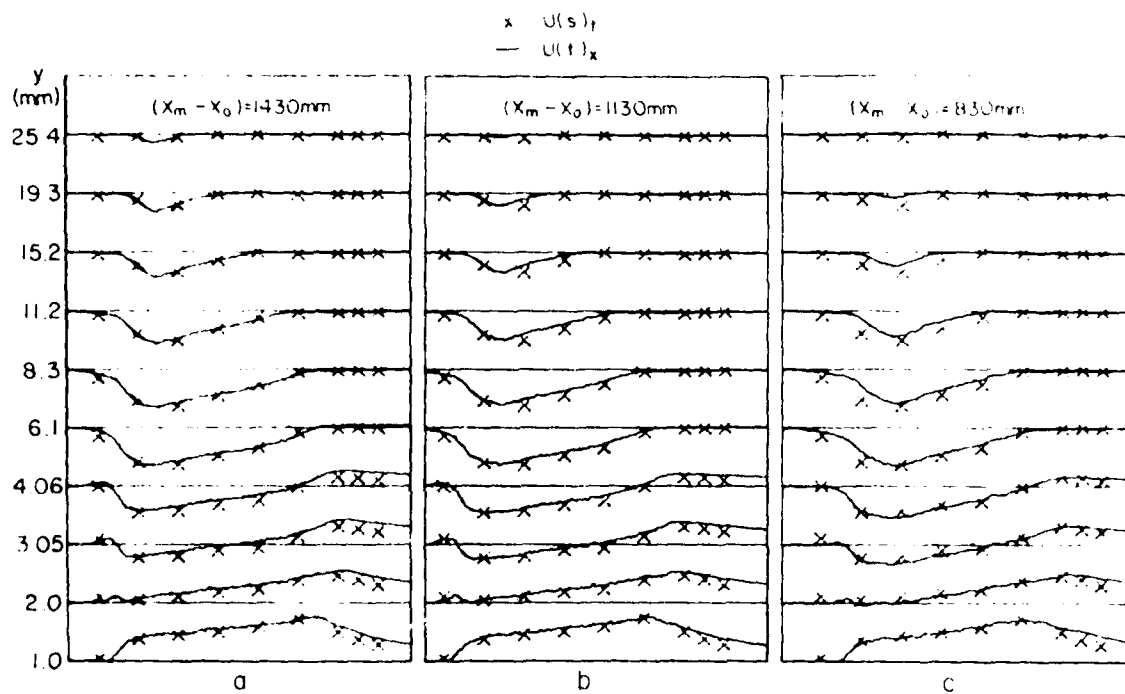
- Fig. 1 (a) An elevation view of spot tagged by dye.  
 (b) A plan view of a spot (courtesy of M. Gad-el-Hak).
- Fig. 2 A single record of velocity perturbation across the spot at  $X_m - X_o = 1030\text{mm}$ ,  $Z = 0$ ,  $U_\infty = 10\text{m/sec}$ ,  $X_s = 300\text{mm}$ .
- Fig. 3 An ensemble-averaged velocity perturbation across the spot at  $X_m - X_o = 1030$ ,  $Z = 0$ ,  $U_\infty = 10\text{m/sec}$ ,  $X_s = 300\text{mm}$ .
- Fig. 4 (a) The determination of the celerity of some distinguished features of the spot  $U_\infty = 10\text{m/sec}$   $X_s = 300\text{mm}$ .  
 (b) Perturbation contours  $(U - U_{LAM})/U_\infty = -2\%$  plotted in  $Y, t$  coordinates.
- Fig. 5 A comparison between a temporal velocity perturbation record at a fixed measuring station with spatial velocity perturbation record at a fixed time.  $U_\infty = 10\text{m/sec}$   $X_s = 300\text{mm}$ .
- Fig. 6 Perturbation contours  $(U - U_{LAM})/U_\infty = \pm 2\%$  plotted in the similarity coordinates suggested  $U_\infty = 10\text{m/sec}$   $X_s = 300\text{mm}$ .  
 (a) Virtual origin obtained from loci 1 and 4 and accounting for  $\delta_{LS}$ .  
 (b) Virtual origin at the location of the spark.  
 (c) Virtual origin obtained from locus 3 with  $\delta_{LS}$  correction included.
- Fig. 7 Perturbation contours  $(U - U_{LAM})/U_\infty = \pm 10\%$  plotted in the similarity coordinates  $U_\infty = 10\text{m/sec}$   $X_s = 300\text{mm}$ .
- Fig. 8 Perturbation contours  $(U - U_{LAM})/U_\infty = \pm 2\%$  plotted in the coordinates suggested by CCD.

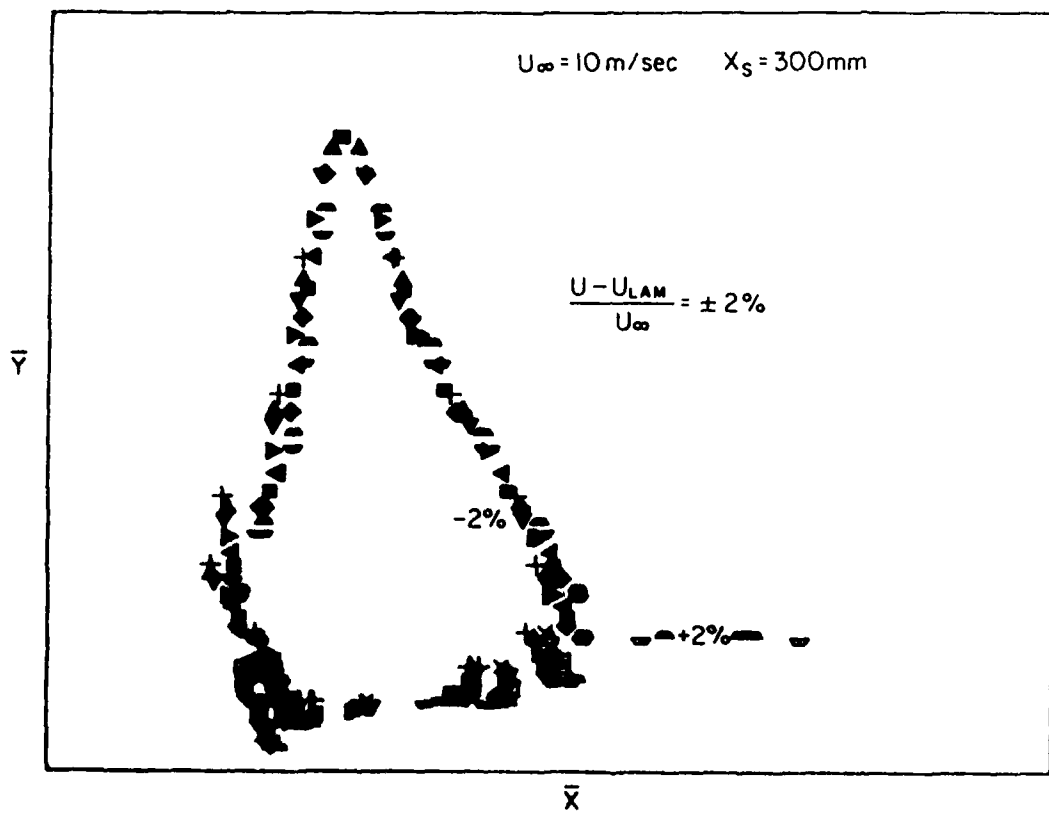
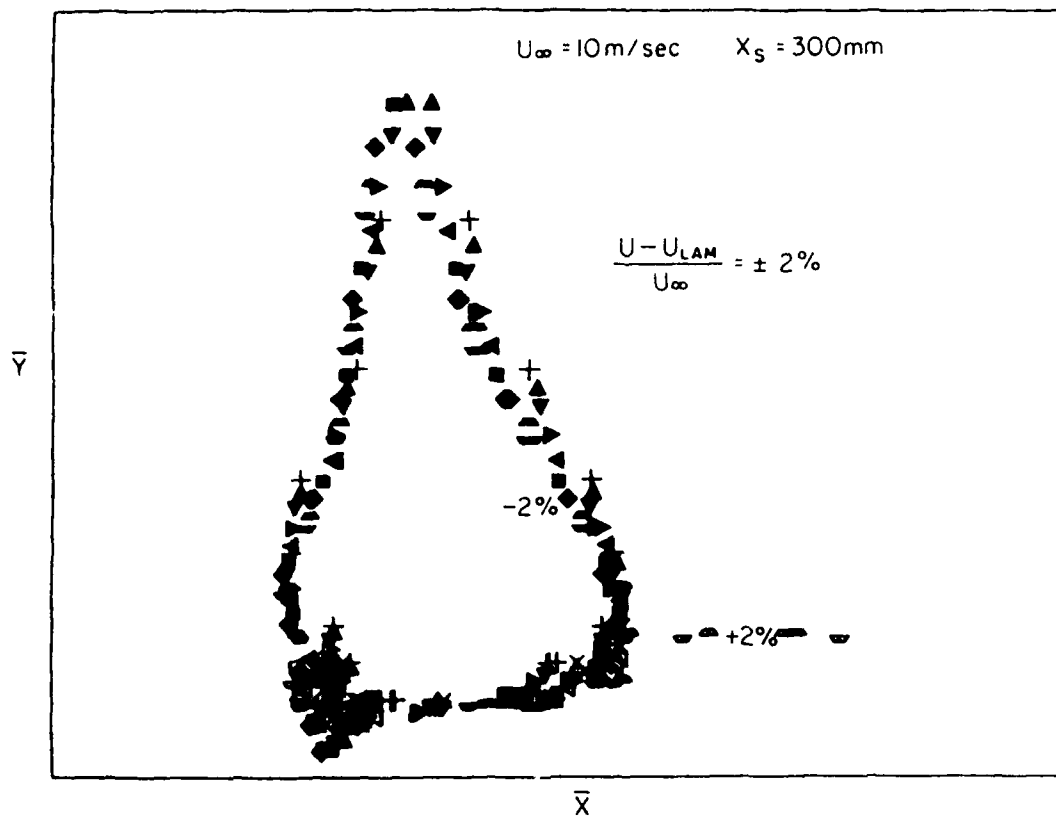
- Fig. 9 Details of velocity perturbation contours measured at  $X_m - X_o = 930\text{mm}$   $U_\infty = 10\text{m/sec}$ .
- Fig. 10 (a) The streamlines relative to an observer moving with the leading interface  $X_m - X_o = 930\text{mm}$   $U_\infty = 10\text{m/sec}$ .  
 (b) The streamlines relative to an observer moving with the trailing interface  $X_m - X_o = 930\text{mm}$   $U_\infty = 10\text{m/sec}$ .
- Fig. 11 The celerity of some distinguished features of the spot measured at  $U_\infty = 19\text{m/sec}$   $X_s = 300\text{mm}$ .
- Fig. 12 The longitudinal rate of growth of the spot and the dependence of  $U_{TE}$  on  $Re_{\delta^*}^s$ .
- Fig. 13 The spanwise  $^s$  growth of the spot for various  $Re_{\delta^*}^s$ .
- Fig. 14 (a) The border of an ensemble-averaged spot at  $U_\infty = 6\text{m/sec}$   $X_s = 300\text{mm}$ .  
 (b) Perturbation contours of -2%; -10%; -20% of an ensemble-averaged spot plotted in similarity coordinates ( $U_\infty = 19\text{m/sec}$   $X_s = 300\text{mm}$ ).
- Fig. 15 (a) Velocity perturbation at  $U_\infty = 6\text{m/sec}$   $X_m - X_o = 1000\text{mm}$ .  
 (b) Velocity perturbation at  $U_\infty = 19\text{m/sec}$   $X_m - X_o = 1000\text{mm}$ .
- Fig. 16 A single record of velocity perturbation measured at  $U_\infty = 6\text{m/sec}$   $X_m - X_o = 940\text{mm}$ .
- Fig. 17 Velocity perturbation contours corresponding to the record shown in Figure 16.

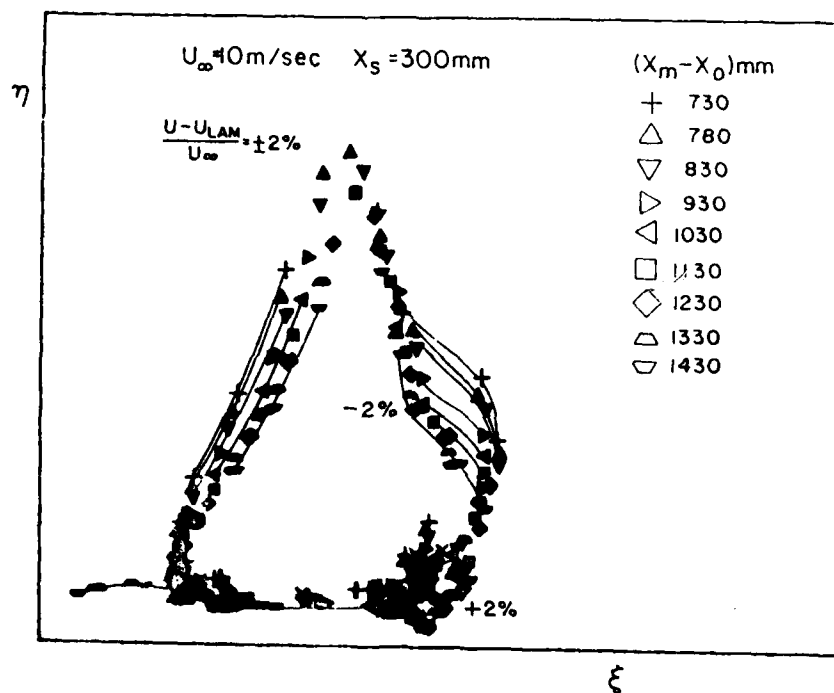
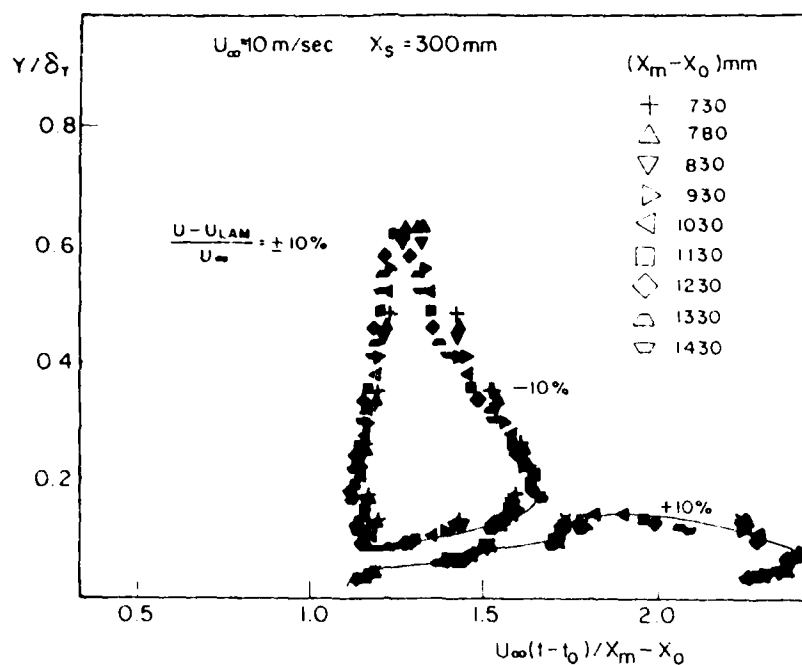


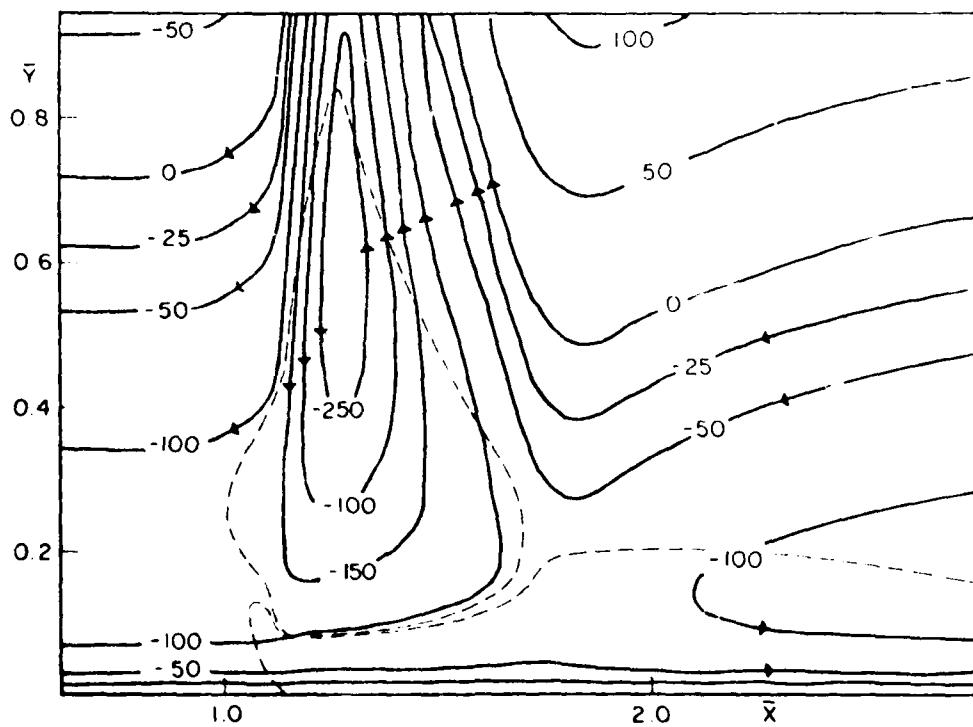
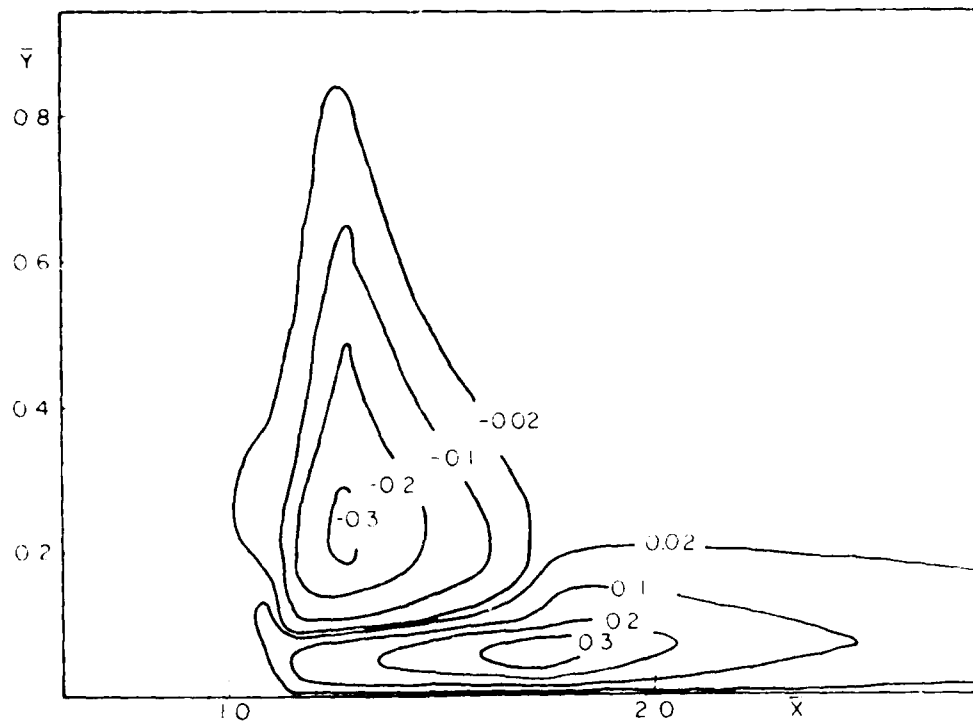


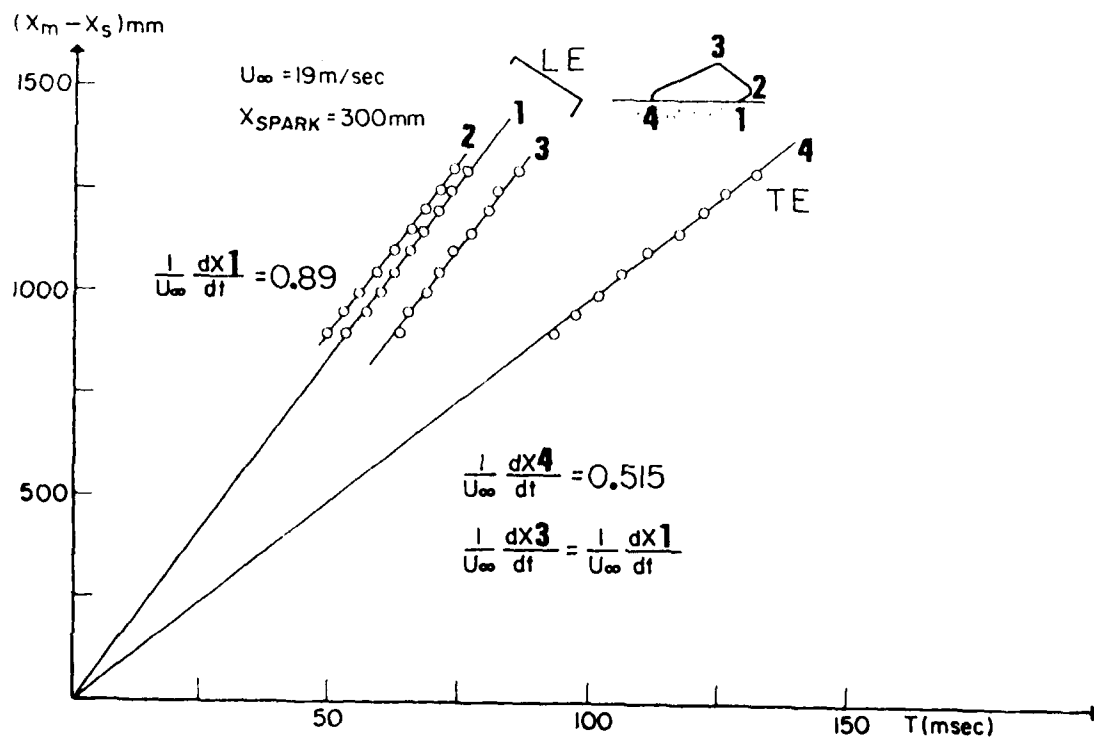
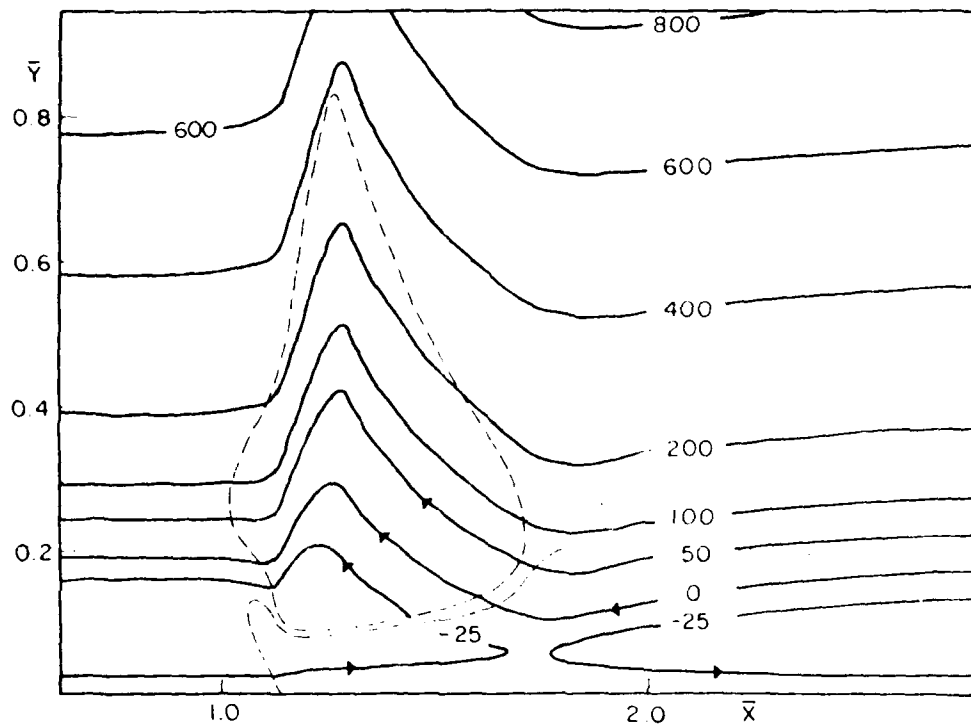


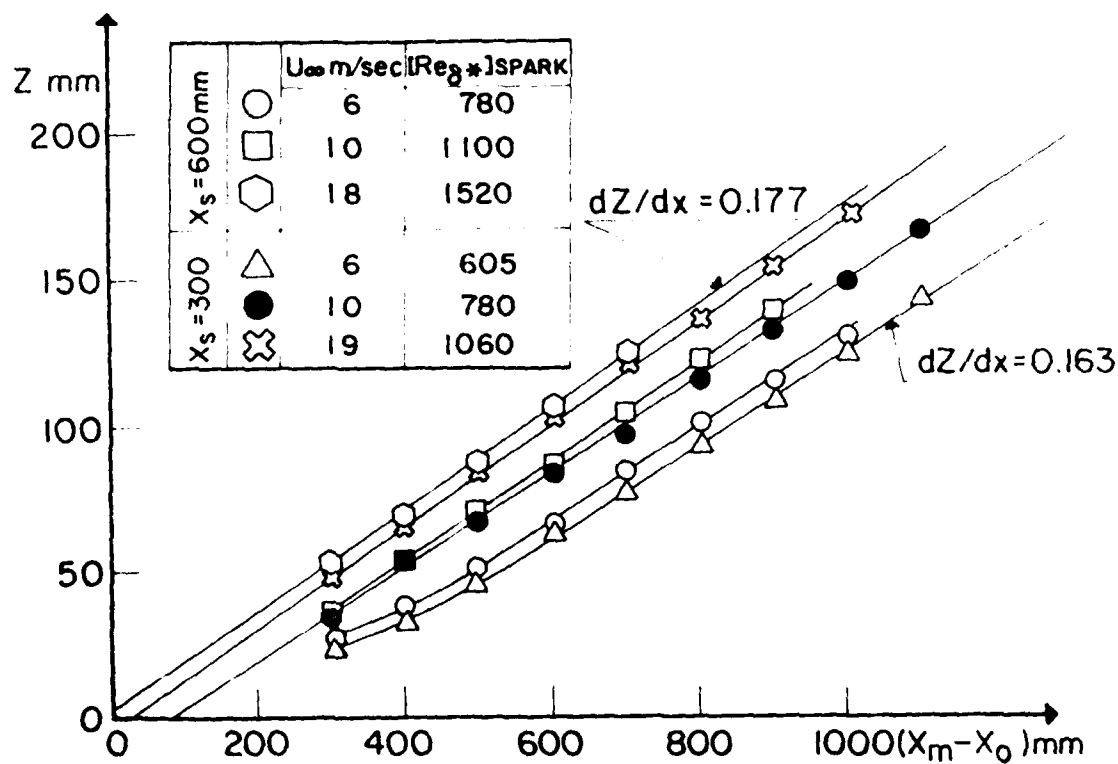
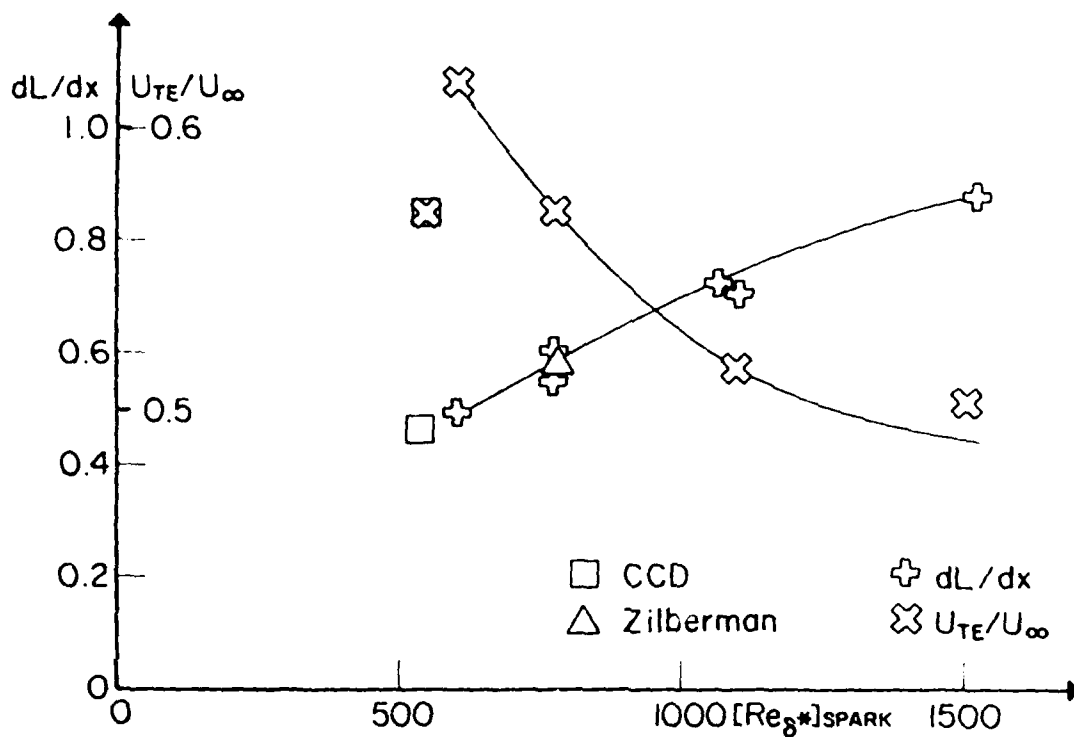


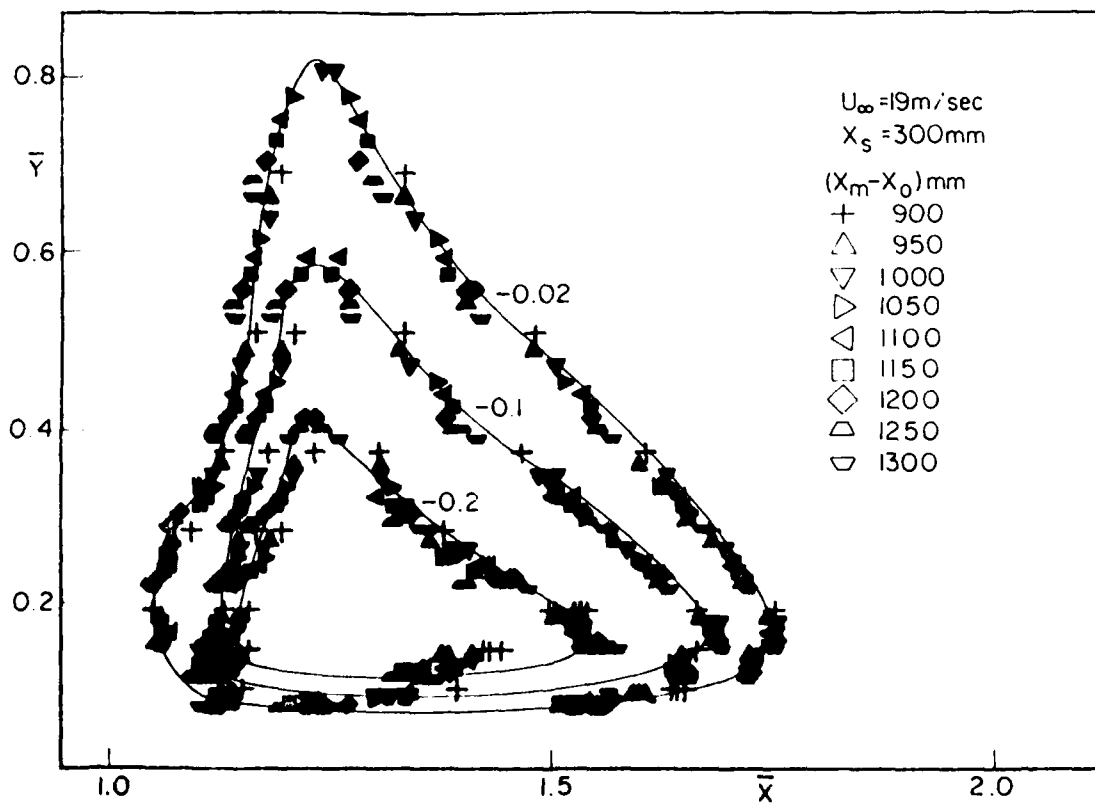
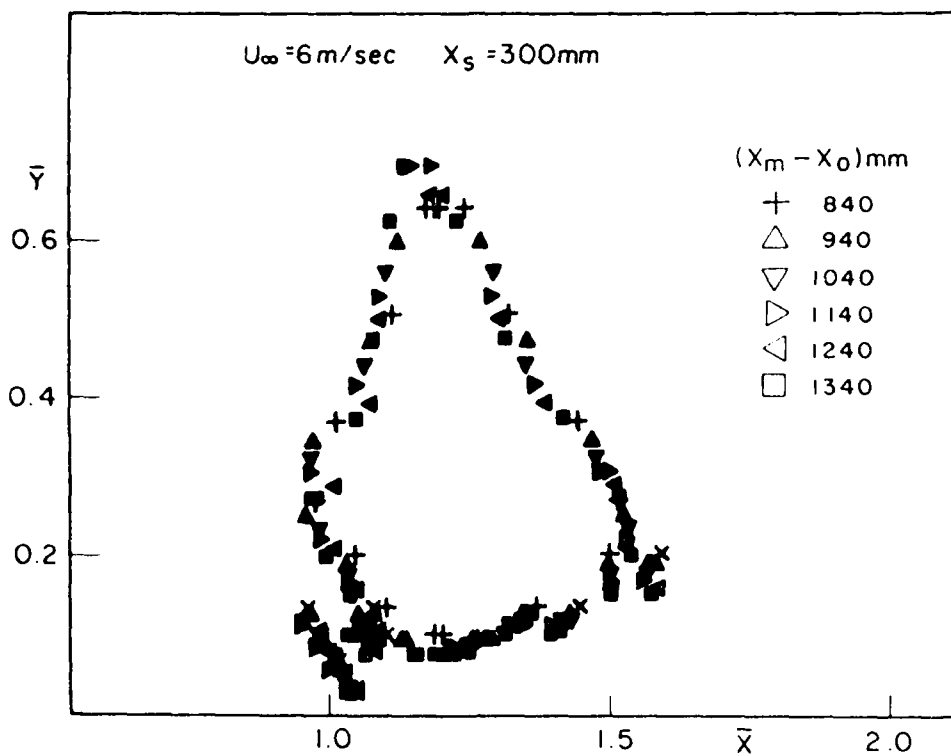


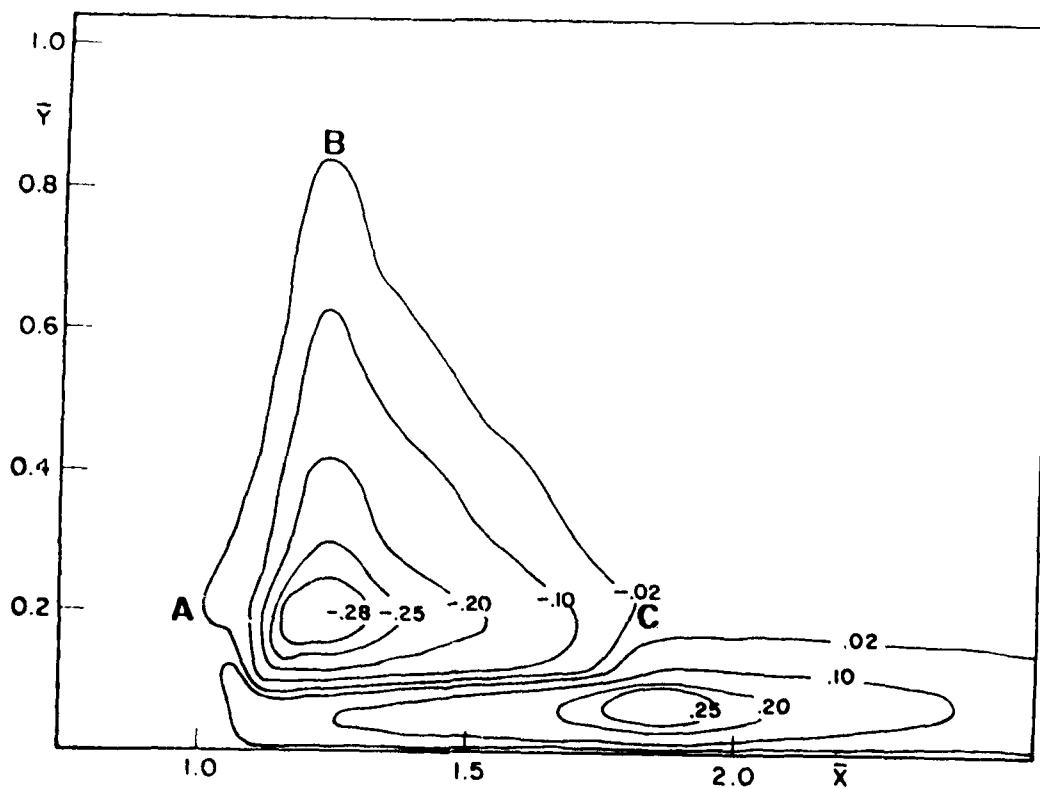
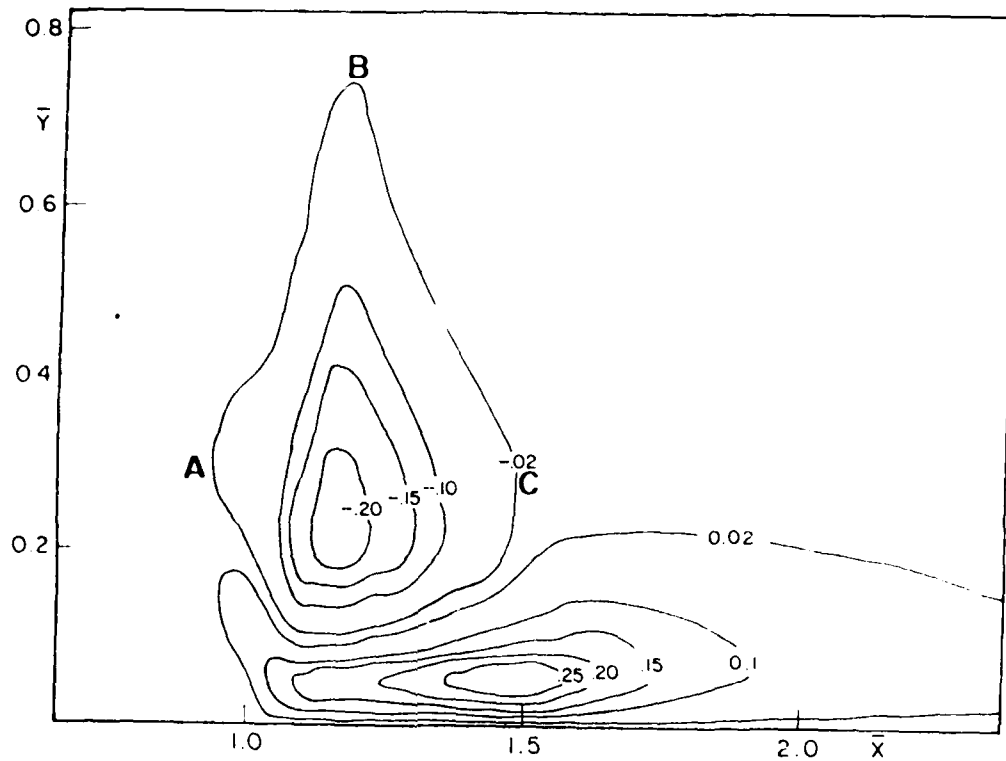


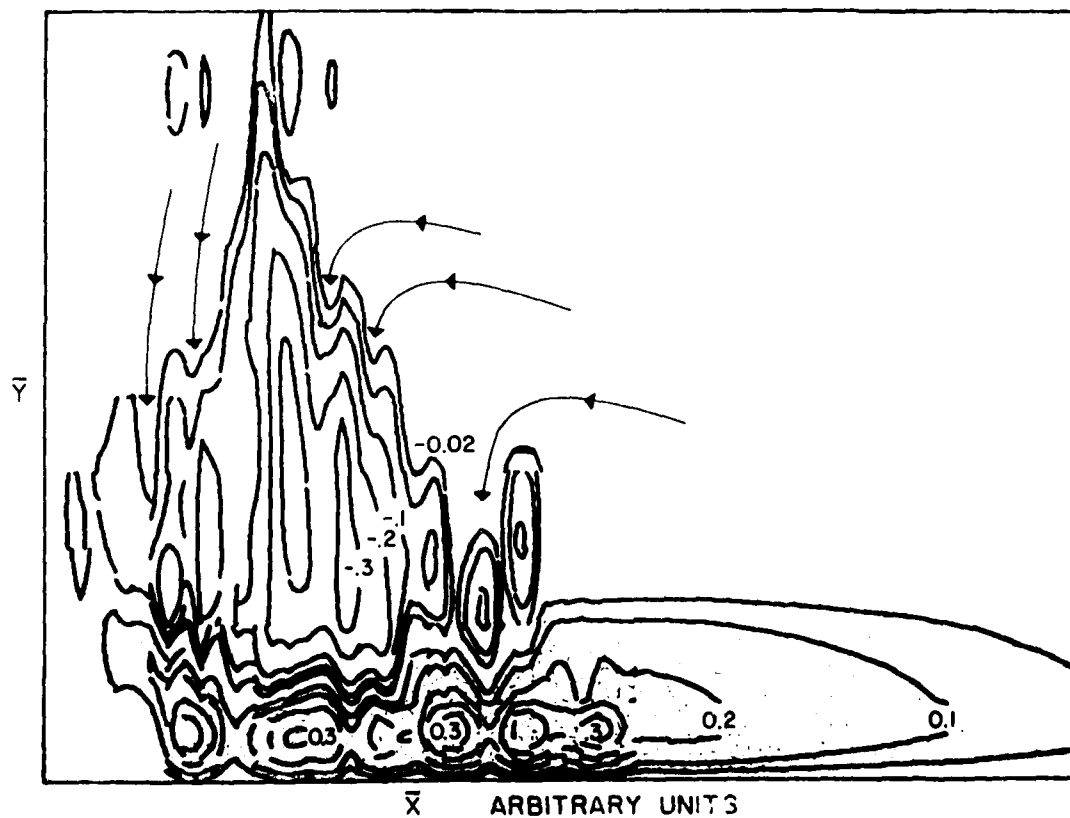
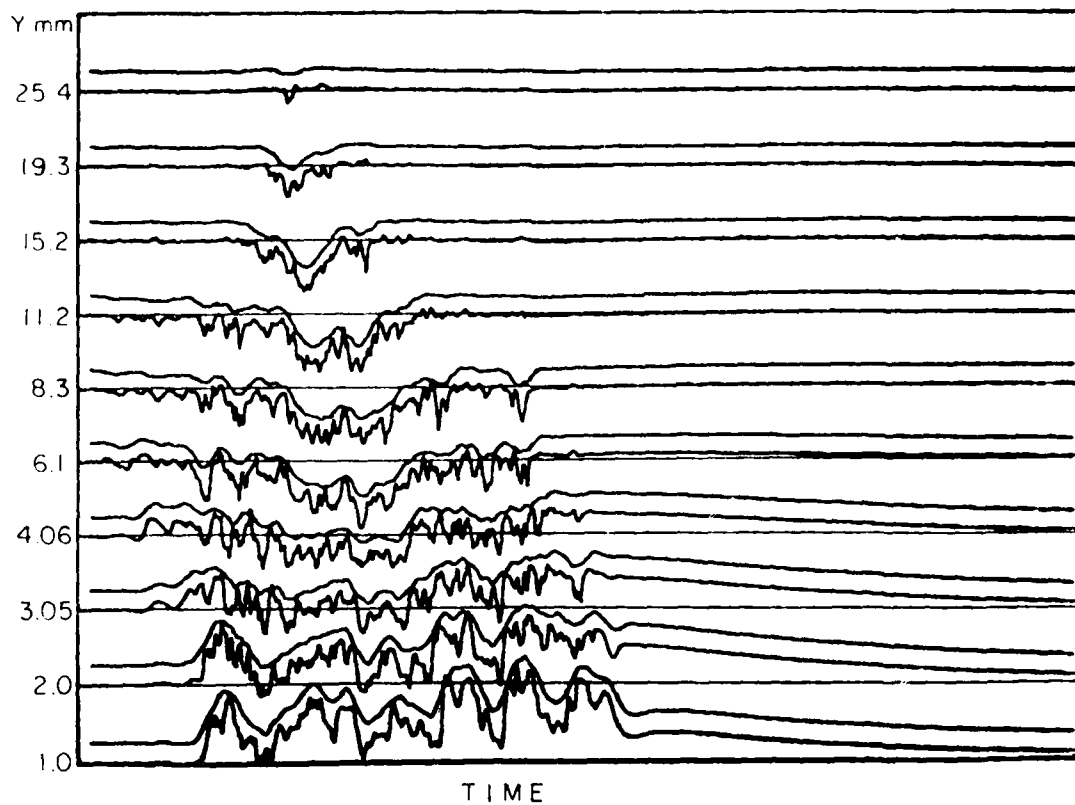












UNCLASSIFIED

SECURITY CLASSIFICATION OF THIS PAGE (When Data Entered)

REPORT DOCUMENTATION PAGE		READ INSTRUCTIONS BEFORE COMPLETING FORM
1. REPORT NUMBER <b>AEOSR-TR- 80-0472</b>	2. GOVT ACCESSION NO. <b>AD-A086 445</b>	3. RECIPIENT'S CATALOG NUMBER
4. TITLE (and Subtitle)  ON THE SPREADING RATE AND STRUCTURE OF A TURBULENT SPOT	5. TYPE OF REPORT & PERIOD COVERED INTERIM 3 Mar 79 - 28 Feb 80	
	6. PERFORMING ORG. REPORT NUMBER	
7. AUTHOR(s)  I WYGNANSKI J HARITONIDIS	8. CONTRACT OR GRANT NUMBER(s)  AFOSR-77-3275	
9. PERFORMING ORGANIZATION NAME AND ADDRESS TEL-AVIV UNIVERSITY SCHOOL OF ENGINEERING RAMAT-AVIV, ISRAEL	10. PROGRAM ELEMENT, PROJECT, TASK AREA & WORK UNIT NUMBERS 2307A2 61102F	
11. CONTROLLING OFFICE NAME AND ADDRESS  AIF FORCE OFFICE OF SCIENTIFIC RESEARCH/NA BUILDING 410 BOLLING AFB, DC 20332	12. REPORT DATE 1 April 1980	
	13. NUMBER OF PAGES 31	
14. MONITORING AGENCY NAME & ADDRESS (if different from Controlling Office)	15. SECURITY CLASS. (of this report)  UNCLASSIFIED	
	15a. DECLASSIFICATION DOWNGRADING SCHEDULE	
16. DISTRIBUTION STATEMENT (of this Report)  Approved for public release; distribution unlimited		
17. DISTRIBUTION STATEMENT (of the abstract entered in Block 20, if different from Report)		
18. SUPPLEMENTARY NOTES		
19. KEY WORDS (Continue on reverse side if necessary and identify by block number)  TRANSITION BOUNDARY LAYER HOT WIRE ANEMOMETRY		
20. ABSTRACT (Continue on reverse side if necessary and identify by block number) Velocity measurements in the plane of symmetry of a turbulent spot are reported. The number of data points taken at various streamwise locations was adequate to map the ensemble-averaged flow field in a spot at a given instance. These results are compared to velocity taken in laboratory coordinates (i.e., at a given station with variable time), whereupon it is shown that the flow field in the spot depends either on its distance from its origin or on the time elapsed from its initiation. The two variables are not independent, so the flow may be transformed into a time (space) independent problem. The dependence of the		

UNCLASSIFIED

SECURITY CLASSIFICATION OF THIS PAGE(When Data Entered)

spot on the Reynolds number and on the surrounding laminar boundary layer is established. The effects of these parameters on the shape of the ensemble averaged spot, its size, characteristic celerities, and relative rate of entrainment, are discussed.

UNCLASSIFIED